

Next-to-leading-order corrections to $B \rightarrow \pi$ form factors in k_T factorization

Hsiang-nan Li^{a,b,c}, Yue-Long Shen^d, Yu-Ming Wang^e

^a*Institute of Physics, Academia Sinica,
Taipei, Taiwan 115, Republic of China*

^b*Department of Physics, National Cheng-Kung University,
Tainan, Taiwan 701, Republic of China*

^c*Department of Physics, National Tsing-Hua University,
Hsinchu, Taiwan 300, Republic of China*

^d*College of Information Science and Engineering,
Ocean University of China, Qingdao,
Shandong 266100, P.R. China*

^e*Theoretische Elementarteilchenphysik,
Naturwissenschaftlich Techn. Fakultät*

Universität Siegen, 57068 Siegen, Germany

(Dated: September 11, 2018)

We calculate next-to-leading-order (NLO) corrections to the $B \rightarrow \pi$ transition form factors at leading twist in the k_T factorization theorem. Light partons off-shell by k_T^2 are considered in the quark diagrams, in the effective diagrams for the B meson wave function defined with the effective heavy-quark field, and in the effective diagrams for the pion wave function. It is explicitly demonstrated that the infrared logarithms $\ln k_T^2$ cancel between the above sets of diagrams, as deriving the k_T -dependent NLO hard kernel from their difference. The infrared finiteness of the hard kernel confirms the application of the k_T factorization theorem to B meson semileptonic decays. The NLO pion wave function is identical to those constructed from the pion transition and electromagnetic form factors, consistent with its universality. Choosing the renormalization and factorization scales lower than the B meson mass, the NLO corrections are under control: they amount only up to 30% of the form factors at large recoil of the pion, when varying models for the meson wave functions.

PACS numbers: 12.38.Bx, 12.38.Cy, 12.39.St, 13.20.He

I. INTRODUCTION

B meson transition form factors are an essential input of the factorization approaches to nonleptonic two-body B meson decays, such as the perturbative QCD (PQCD) approach [1, 2] based on the k_T factorization theorem [3–8]. For next-to-leading-order (NLO) contributions in leading-twist PQCD, the vertex corrections, the quark loops, and the magnetic penguins associated with the weak decay vertices in factorizable emission amplitudes have been calculated [9–11]. As explained in [9], the above corrections may be the most crucial NLO pieces for understanding the known $B \rightarrow \pi\pi$ and $B \rightarrow \pi K$ puzzles, which result from the large observed $\pi^0\pi^0$ branching ratio, and from the dramatically different direct CP asymmetries between the $\pi^\mp K^\pm$ and $\pi^0 K^\pm$ modes, respectively. There have been many applications of this NLO PQCD formalism to nonleptonic two-body B and B_s meson decays in the literature. For NLO corrections to spectator diagrams, we have identified the so-called Glauber divergences, in addition to those which are absorbed into hadron wave functions, and summed them into a phase factor to all orders [12]. It was observed that the phase factor modifies the interference pattern between the spectator diagrams, and further improves the resolution of the $B \rightarrow \pi\pi$, πK puzzles in NLO PQCD. At the same level of accuracy, we need to calculate NLO corrections to the B meson transition form factors for completeness.

In this paper we shall extend the NLO framework for the pion electromagnetic form factor in the k_T factorization [13] to the $B \rightarrow \pi$ transition form factors. In this framework light partons in both QCD quark diagrams and effective diagrams for hadron wave functions are off mass shell by k_T^2 [14, 15]. Not only the collinear divergences from gluon emissions collimated to the pion, but also the soft divergences from gluon exchanges between the two mesons exist. Compared to the pion form factor [13], a new point is that an infrared regulator associated with the b quark is not needed. Due to its finite mass, gluons radiated by the b quark do not generate collinear divergences. Soft divergences can be regularized either by the virtuality of internal particles, or by the virtuality k_T^2 of other light partons, to which the radiative gluons attach. That is, the b quark remains on-shell in the above framework, a condition which justifies the approximation of the b quark field by the effective heavy-quark field for defining the B meson wave function. The NLO pion wave function is found to be identical to those constructed in the pion electromagnetic and transition form factors [13, 15], consistent with its universality. Note that the diagrams considered here differ from those in the

QCD-improved factorization (QCDF) approach [16] and in the soft-collinear effective theory (SCET) [17], which are based on the collinear factorization theorem [18]: there is no end-point singularity in the k_T factorization, so it is not necessary to introduce soft form factors [19] or to perform the zero-bin subtraction [20] in our calculation.

It will be demonstrated that the collinear and soft divergences in the quark diagrams are cancelled by those in the effective diagrams for the B meson and pion wave functions. Taking the difference of the above sets of diagrams, we derive the k_T -dependent NLO hard kernel at leading twist for the $B \rightarrow \pi$ transition form factors. The infrared finiteness of the hard kernel confirms the application of the k_T factorization theorem to B meson semileptonic decays [21]. Similar to the analysis in [13, 15], both the large double logarithms $\alpha_s \ln^2 k_T$ and $\alpha_s \ln^2 x$, x being a parton momentum fraction, are identified. The former is absorbed into the B meson and pion wave functions and summed to all orders in the coupling constant α_s by the k_T resummation [1], and the latter is absorbed into a jet function and summed to all orders by the threshold resummation [22]. Due to the dominant soft dynamics associated with the b quark, the effect of the k_T resummation from the B meson side is minor. The renormalization scale μ and the factorization scale μ_f are introduced by higher-order corrections to the quark diagrams and to the effective diagrams, respectively. Choosing μ and μ_f appropriately, with both being lower than the B meson mass as postulated in [2, 7], the NLO corrections are under control: they amount only up to 30% of the form factors at large recoil of the pion, when varying models for the meson wave functions.

In Sec. II we calculate the $O(\alpha_s^2)$ QCD quark diagrams for the $B \rightarrow \pi \ell \bar{\nu}$ semileptonic decay, the $O(\alpha_s)$ effective diagrams for the B meson and pion wave functions, and their convolutions with the $O(\alpha_s)$ hard kernel. Since the k_T factorization is appropriate for QCD processes dominated by contributions from small x [14], we shall keep only terms in leading power of x . The important double logarithms are identified, and the k_T -dependent NLO hard kernel is presented. Section III contains the numerical investigation, in which we examine the dependence of the NLO contributions to the $B \rightarrow \pi$ transition form factors on the renormalization and factorization scales, and on the shape of the B meson and pion wave functions. Section IV is the conclusion.

II. NLO CORRECTIONS

In this section we calculate the $O(\alpha_s^2)$ quark diagrams for the $B \rightarrow \pi \ell \bar{\nu}$ semileptonic decay, and the $O(\alpha_s)$ effective diagrams for the B meson and pion wave functions in the Feynman gauge. The $B \rightarrow \pi$ transition form factors are defined via the matrix element

$$\langle \pi(P_2) | \bar{u} \gamma^\mu b | B(P_1) \rangle = f^+(q^2)(P_1^\mu + P_2^\mu) + [f^0(q^2) - f^+(q^2)] \frac{m_B^2 - m_\pi^2}{q^2} q^\mu, \quad (1)$$

where m_B (m_π) is the B meson (pion) mass, and $q = P_1 - P_2$ is the transfer momentum. The momentum P_1 (P_2) of the B meson (pion) is chosen as $P_1 = P_1^+(1, 1, \mathbf{0}_T)$ ($P_2 = (0, P_2^-, \mathbf{0}_T)$) with the component $P_1^+ = m_B/\sqrt{2}$ ($P_2^- = \eta m_B/\sqrt{2}$). The large recoil region of the pion corresponds to the energy fraction $\eta \sim O(1)$. According to the k_T factorization, the anti-quark \bar{q} carries the momentum $k_1 = (x_1 P_1^+, 0, \mathbf{k}_{1T})$ in the B meson and $k_2 = (0, x_2 P_2^-, \mathbf{k}_{2T})$ in the pion, x_1 and x_2 being the momentum fractions, as labelled in the leading-order (LO) quark diagrams in Fig. 1. We postulate the hierarchy

$$m_B^2 \gg x_2 m_B^2 \gg x_1 m_B^2 \gg x_1 x_2 m_B^2, k_{1T}^2, k_{2T}^2, \quad (2)$$

in the small- x region, which is roughly consistent with the order of magnitude: $x_2 \sim 0.3$, $x_1 \sim 0.1$, $m_B \sim 5$ GeV, and $k_T \lesssim 1$ GeV. Under the above hierarchy, only those terms that do not vanish in the $x \rightarrow 0$ and $k_T \rightarrow 0$ limits are kept, so the expressions of our NLO results will be greatly simplified.

To obtain the LO hard kernels, we sandwich Fig. 1 with the following leading-twist spin projectors for the B meson and the pion [16, 23]

$$\frac{1}{2\sqrt{N_c}} (P_1 + m_B) \gamma_5 \left[\not{n}_+ \phi_B^{(+)}(x_1) + \left(\not{n}_- - k_1^+ \gamma_\perp^\nu \frac{\partial}{\partial \mathbf{k}_{1T}^\nu} \right) \phi_B^{(-)}(x_1) \right], \quad \frac{1}{\sqrt{2N_c}} \gamma_5 P_2 \phi_\pi(x_2), \quad (3)$$

respectively, where the dimensionless vectors are defined by $n_+ = (1, 0, \mathbf{0}_T)$, and $n_- = (0, 1, \mathbf{0}_T)$ along P_2 , and N_c is the number of colors. The contributions proportional to the B meson distribution amplitudes $\phi_B^{(+)}$ and $\phi_B^{(-)}$ from Fig. 1(a) are computed as

$$H_a^{(0)}(x_1, k_{1T}, x_2, k_{2T}) = -4g^2 C_F \frac{[x_2 \eta \phi_B^{(+)}(x_1) + \phi_B^{(-)}(x_1)] P_2^\mu}{x_2 \eta (x_1 x_2 \eta m_B^2 + |\mathbf{k}_{1T} - \mathbf{k}_{2T}|^2)} \phi_\pi(x_2), \quad (4)$$

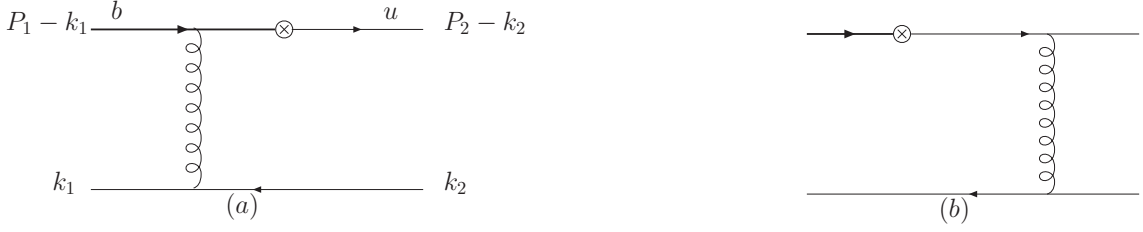


FIG. 1: Leading-order quark diagrams for the $B \rightarrow \pi$ transition form factors with \otimes representing the weak vertex.

with the strong coupling g , and the color factor C_F . To reach the above expression, we have applied the hierarchy $x_2 m_B^2 \gg k_{2T}^2$ in Eq. (2) to the internal b quark propagator. The denominator $x_1 x_2 \eta m_B^2 + |\mathbf{k}_{1T} - \mathbf{k}_{2T}|^2$ comes from the virtuality of the LO hard gluon, in which the $|\mathbf{k}_{1T} - \mathbf{k}_{2T}|^2$ term smears the end-point singularity from small x_2 . Similarly, Fig. 1(b) leads to the amplitude

$$H_b^{(0)}(x_1, k_{1T}, x_2, k_{2T}) = -4g^2 C_F \frac{(\eta P_1^\mu - P_2^\mu) \phi_B^{(+)}(x_1) + P_2^\mu \phi_B^{(-)}(x_1)}{\eta(x_1 x_2 \eta m_B^2 + |\mathbf{k}_{1T} - \mathbf{k}_{2T}|^2)} \phi_\pi(x_2). \quad (5)$$

Comparing Eqs. (4) and (5), it is easy to see that the term proportional to $\phi_B^{(-)}$ from Fig. 1(a) dominates numerically according to the hierarchy in Eq. (2). As explained above, the $B \rightarrow \pi$ form factors receive major contributions from the small- x region, in which the k_T factorization is an appropriate framework. Since the amplitude from Fig. 1(b) is suppressed by a power of x_2 , we will not consider the NLO corrections to $H_b^{(0)}(x_1, k_{1T}, x_2, k_{2T})$, and focus on those to Fig. 1(a) below. The term proportional to P_1^μ in Eq. (5) gives the symmetry breaking effect [16], which is calculable even in the collinear factorization, as convoluted with $\phi_B^{(+)}(x_1) \sim x_1$ at small x_1 .

A. NLO Quark Diagrams

The NLO corrections to Fig. 1(a) contain Figs. 2, 3, and 4 for the self-energy corrections, the vertex corrections, and the box and pentagon diagrams, respectively. The ultraviolet poles are extracted in the dimensional reduction [24] in order to avoid the ambiguity from handling the matrix γ_5 . We adopt the following convenient dimensionless ratios

$$\begin{aligned} \delta_1 &= \frac{k_{1T}^2}{m_B^2}, & \delta_2 &= \frac{k_{2T}^2}{m_B^2}, \\ \delta_{12} &= \frac{x_1 x_2 \eta m_B^2 + |\mathbf{k}_{1T} - \mathbf{k}_{2T}|^2}{m_B^2}, \end{aligned} \quad (6)$$

as presenting our results. The infrared poles are then identified as the logarithms $\ln \delta_1$ and $\ln \delta_2$.

The self-energy corrections in Fig. 2 give

$$G_{2a}^{(1)} = -\frac{\alpha_s C_F}{4\pi} \left[\frac{6}{\delta_1} \left(\frac{1}{\epsilon} + \ln \frac{4\pi\mu^2}{m_B^2 e^{\gamma_E}} + \frac{5}{3} \right) + \frac{1}{2} \left(\frac{1}{\epsilon} + \ln \frac{4\pi\mu^2}{m_B^2 e^{\gamma_E}} + 2 \ln \frac{m_g^2}{m_B^2} - 1 \right) \right] H^{(0)}, \quad (7)$$

$$G_{2b}^{(1)} = -\frac{\alpha_s C_F}{8\pi} \left[\frac{1}{\epsilon} + \ln \frac{4\pi\mu^2}{\delta_1 m_B^2 e^{\gamma_E}} + 2 \right] H^{(0)}, \quad (8)$$

$$G_{2c,2d}^{(1)} = -\frac{\alpha_s C_F}{8\pi} \left[\frac{1}{\epsilon} + \ln \frac{4\pi\mu^2}{\delta_2 m_B^2 e^{\gamma_E}} + 2 \right] H^{(0)}, \quad (9)$$

$$G_{2e}^{(1)} = -\frac{\alpha_s C_F}{4\pi} \left[\frac{6}{x_2 \eta} \left(\frac{1}{\epsilon} + \ln \frac{4\pi\mu^2}{m_B^2 e^{\gamma_E}} + \frac{5}{3} \right) + \left(\frac{1}{\epsilon} + \ln \frac{4\pi\mu^2}{m_B^2 e^{\gamma_E}} + 4 \ln(x_2 \eta) - 5 \right) \right] H^{(0)}, \quad (10)$$

$$G_{2f+2g+2h+2i}^{(1)} = \frac{\alpha_s}{4\pi} \left[\left(\frac{5}{3} N_c - \frac{2}{3} N_f \right) \left(\frac{1}{\epsilon} + \ln \frac{4\pi\mu^2}{\delta_{12} m_B^2 e^{\gamma_E}} \right) \right] H^{(0)}, \quad (11)$$

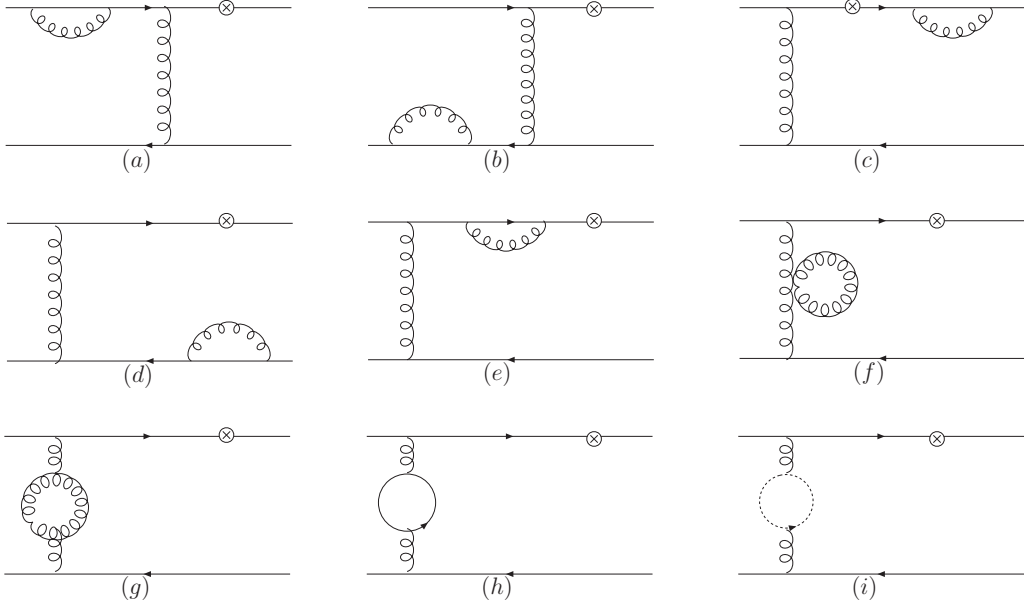


FIG. 2: Self-energy corrections to Fig. 1(a).

where $1/\epsilon$ represents the ultraviolet pole, μ is the renormalization scale, γ_E is the Euler constant, N_f is the number of quark flavors, and $H^{(0)}$ denotes the leading-twist LO hard kernel proportional to P_2^μ ,

$$H^{(0)}(x_1, k_{1T}, x_2, k_{2T}) = -\frac{4g^2 C_F P_2^\mu}{x_2 \eta \delta_{12} m_B^2}. \quad (12)$$

The above expressions are basically similar to the corresponding ones obtained in the pion electromagnetic form factor [13]. We emphasize only that Fig. 2(a), the self-energy correction to the b quark, requires a mass renormalization as indicated by the first term in the square brackets of Eq. (7). The finite piece of the first term is then absorbed, with the relation $(P_1 - k_1)^2 - m_b^2 = -k_{1T}^2$, into the redefinition the b quark mass,

$$\frac{1}{(P_1 - k_1)^2 - m_b^2} \left[1 - \frac{\alpha_s C_F}{4\pi} \frac{6}{\delta_1} \left(\ln \frac{\mu^2}{m_B^2} + \frac{5}{3} \right) \right] = \frac{1}{(P_1 - k_1)^2 - m_b^2(\mu)}, \quad (13)$$

leading to the pole mass

$$m_b(\mu) = m_b \left[1 + \frac{\alpha_s}{\pi} \left(\ln \frac{\mu^2}{m_B^2} + \frac{5}{3} \right) \right]. \quad (14)$$

In this work we shall not differentiate $m_b(\mu)$ from m_B , because the distinction between them contributes at next-to-leading power. The second term in the square brackets of Eq. (7) represents the correction to the b quark wave function. As explained before, we shall consider an on-shell valence b quark, so the involved soft divergence is regularized by a gluon mass m_g , which will be cancelled by the corresponding soft divergence in the effective diagram Fig. 5(a) below.

The results from the vertex corrections in Fig. 3 are summarized as

$$G_{3a}^{(1)} = \frac{\alpha_s C_F}{4\pi} \left[\frac{1}{\epsilon} + \ln \frac{4\pi\mu^2}{m_B^2 e^{\gamma_E}} - 2 \ln \left(\frac{\delta_2}{\eta} \right) (1 + \ln x_2) + \ln^2 x_2 - \frac{\pi^2 - 3}{2} \right] H^{(0)}, \quad (15)$$

$$G_{3b}^{(1)} = -\frac{\alpha_s}{8\pi N_c} \left[\frac{1}{\epsilon} + \ln \frac{4\pi\mu^2}{m_B^2 e^{\gamma_E}} + 4 \ln(x_2 \eta) \right] H^{(0)}, \quad (16)$$

$$G_{3c}^{(1)} = -\frac{\alpha_s}{8\pi N_c} \left[\frac{1}{\epsilon} + \ln \frac{4\pi\mu^2}{\delta_{12} m_B^2 e^{\gamma_E}} - 2 \ln \left(\frac{\delta_1}{\delta_{12}} \right) \ln \left(\frac{\delta_2}{\delta_{12}} \right) - 2 \ln \left(\frac{\delta_1 \delta_2}{\delta_{12}^2} \right) - \frac{2\pi^2}{3} + \frac{9}{2} \right] H^{(0)}, \quad (17)$$

$$G_{3d}^{(1)} = \frac{\alpha_s N_c}{8\pi} \left[\frac{3}{\epsilon} - 3\gamma_E + 3 \ln \frac{4\pi\mu^2}{\delta_{12} m_B^2 e^{\gamma_E}} + 2 \ln \left(\frac{\delta_{12}^2}{\delta_1 \delta_2} \right) + 7 \right] H^{(0)}, \quad (18)$$

$$G_{3e}^{(1)} = \frac{\alpha_s N_c}{8\pi} \left[\frac{3}{\epsilon} + 3 \ln \frac{4\pi\mu^2}{m_B^2 e^{\gamma_E}} - \frac{1}{2} \ln^2 \left(\frac{\delta_{12}}{\eta^2} \right) + 2(\ln x_2 - 1) \ln \left(\frac{x_1}{\eta} \right) - \frac{\pi^2}{2} + 3 \right] H^{(0)}. \quad (19)$$

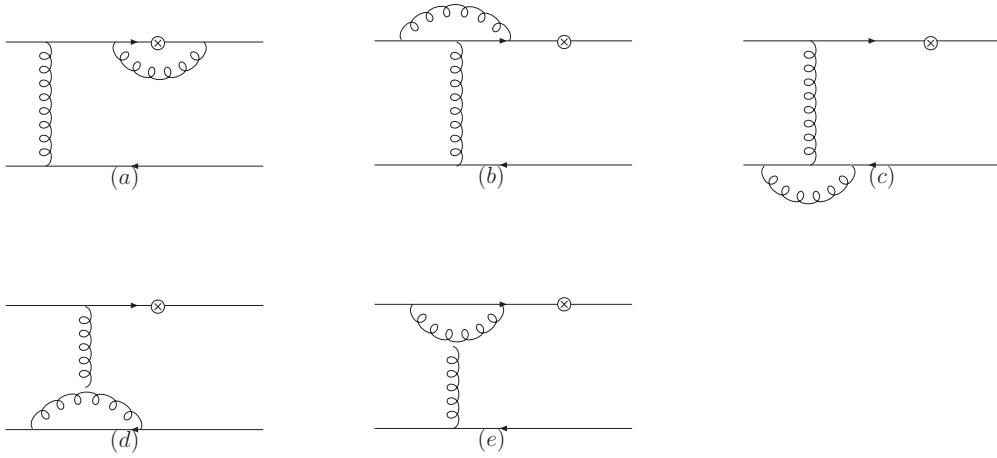


FIG. 3: Vertex corrections to Fig. 1(a).

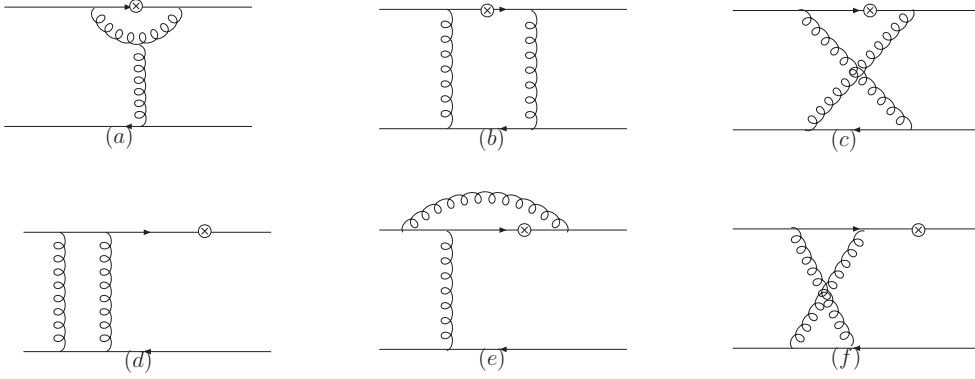


FIG. 4: Box and pentagon diagrams.

The amplitude from Fig. 3(a) depends only on the regulator δ_2 , because the radiative gluon attaches to the virtual b quark line. The double logarithm $2 \ln \delta_2 \ln x_2$ leads to the known Sudakov logarithm $\ln^2 \delta_2$ and the known threshold logarithm $\ln^2 x_2$ [13, 15], as reexpressed in the form

$$2 \ln \delta_2 \ln x_2 = \ln^2 \delta_2 + \ln^2 x_2 - \ln^2 \frac{\delta_2}{x_2}. \quad (20)$$

The radiative gluon in Fig. 3(b) attaches to the massive valence b quark and the virtual b quark, so Eq. (16) is infrared finite. The radiative gluon in Fig. 3(c) attaches to the light valence anti-quarks, such that both the collinear and soft divergences are produced, with the latter being denoted by the product $\ln \delta_1 \ln \delta_2$. This term can be absorbed neither into the B meson wave function nor into the pion wave function. Since the radiative gluon attaches to the virtual LO hard gluon in Fig. 3(d), the soft divergence does not appear Eq. (18). Equations (17) and (18) are symmetric under the exchange of the regulators δ_1 and δ_2 , as they should. Similar to Fig. 3(b), Fig. 3(e) also gives an infrared finite contribution.

The box diagrams and the pentagon diagrams in Fig. 4 lead to the amplitudes

$$G_{4a}^{(1)} = -\frac{\alpha_s N_c}{4\pi} \left[\ln \left(\frac{x_2 \eta^2}{\delta_2} \right) + 1 \right] x_2 H^{(0)}, \quad (21)$$

$$G_{4c}^{(1)} = -\frac{\alpha_s}{4\pi N_c} \left[\ln \left(\frac{x_1 \eta}{\delta_1} \right) \ln \left(\frac{\delta_{12}}{\delta_2} \right) + \frac{\pi^2}{6} \right] H^{(0)}, \quad (22)$$

$$G_{4d}^{(1)} = -\frac{\alpha_s C_F}{4\pi} \left[\ln^2 \left(\frac{\delta_1}{x_1^2} \right) - \ln^2 x_1 - \frac{7\pi^2}{3} \right] H^{(0)}, \quad (23)$$

$$G_{4e}^{(1)} = \frac{\alpha_s}{8\pi N_c} \left[\ln^2 \left(\frac{x_2 \eta^2}{\delta_2} \right) + \pi^2 \right] H^{(0)}, \quad (24)$$

$$G_{4f}^{(1)} = \frac{\alpha_s}{8\pi N_c} \left[\ln \left(\frac{\delta_{12}}{\delta_2} \right) \left(\ln(\delta_{12} \delta_2) - 4 \ln(x_2 \eta) \right) \right] H^{(0)}. \quad (25)$$

Note that Eq. (21) is power-suppressed in the small x_2 region, while the corresponding diagram gives a leading amplitude in the pion form factor [13]. The difference is attributed to the spin projectors: it is $\not{n}_- \propto \gamma^+$ on the B meson side here, but $\not{P}_1 \propto \gamma^-$ on the initial pion side in the latter case. Simply counting the sequence of the gamma matrices, it is easy to understand that Fig. 4(a) does not produce an amplitude proportional to $H^{(0)}$ at leading power. Figure 4(b) is a two-particle reducible diagram, so its contribution will be cancelled by the corresponding effective diagram for the pion wave function [13], and needs not to be computed. Figure 4(c) also contains the soft divergence denoted by the $\ln \delta_1 \ln \delta_2$ term, which cancels that in Fig. 3(c). It seems that Fig. 4(d) generates a collinear divergence, as the gluon on the right is parallel to the light anti-quark in the pion. However, a careful look at the sequence of the gamma matrices, similar to that for Fig. 4(a), reveals power suppression on this collinear divergence. Equation (24) does not depend on an infrared regulator associated with the massive valence b quark, because δ_2 alone is enough to regularize the collinear and soft divergences. The collinear divergence associated with the light valence anti-quark on the B meson side is also power-suppressed in Fig. 4(f), so Eq. (25) does not contain $\ln \delta_1$.

The amplitudes from all the NLO quark diagrams are summed into

$$\begin{aligned} G^{(1)} = & \frac{\alpha_s C_F}{4\pi} \left[\frac{21}{4} \left(\frac{1}{\epsilon} + \ln \frac{4\pi\mu^2}{m_B^2 e^{\gamma_E}} \right) - \ln^2 \delta_1 + \left(4 \ln x_1 - \frac{3}{2} \right) \ln \delta_1 + \ln \frac{m_B^2}{m_g^2} - (2 \ln x_2 + 3) \ln \delta_2 \right. \\ & - \frac{55}{16} \ln^2 x_1 + \frac{7}{16} \ln^2 x_2 + \frac{9}{8} \ln x_1 \ln x_2 + \frac{7 \ln \eta - 18}{8} \ln x_1 + \frac{7 \ln \eta - 36}{8} \ln x_2 \\ & \left. - \frac{\ln \eta (7 \ln \eta + 4)}{16} + \frac{23}{16} \pi^2 + \frac{235}{16} \right] H^{(0)}, \end{aligned} \quad (26)$$

for $N_f = 6$. The ultraviolet pole in the above expression is the same as in the pion electromagnetic form factor, which determines the renormalization-group (RG) evolution of the coupling constant α_s .

B. NLO Effective Diagrams

The $O(\alpha_s)$ B meson wave function $\Phi_B^{(1)}$ [25] and the $O(\alpha_s)$ pion wave function $\Phi_\pi^{(1)}$ [14, 26] collect the effective diagrams from the matrix elements of the leading Fock states

$$\Phi_B(x_1, k_{1T}; x'_1, k'_{1T}) = \int \frac{dz^-}{2\pi} \frac{d^2 z_T}{(2\pi)^2} e^{-ix'_1 P_1^+ z^- + ik'_{1T} \cdot \mathbf{z}_T} \langle 0 | \bar{q}(z) W_z(n_1)^\dagger W_0(n_1) \not{n}_- \Gamma h_v(0) | h_v \bar{q}(k_1) \rangle, \quad (27)$$

$$\begin{aligned} \Phi_\pi(x_2, k_{2T}; x'_2, k'_{2T}) = & \int \frac{dy^+}{2\pi} \frac{d^2 y_T}{(2\pi)^2} e^{-ix'_2 P_2^- y^+ + ik'_{2T} \cdot \mathbf{y}_T} \\ & \times \langle 0 | \bar{q}(y) W_y(n_2)^\dagger W_0(n_2) \not{n}_+ \gamma_5 q(0) | u(P_2 - k_2) \bar{q}(k_2) \rangle, \end{aligned} \quad (28)$$

respectively, with $z = (0, z^-, \mathbf{z}_T)$ and $y = (y^+, 0, \mathbf{y}_T)$ being the coordinates of the anti-quark field \bar{q} , respectively, h_v the effective heavy-quark field, and Γ an appropriate gamma matrix. In the above expressions the Wilson line $W_z(n_1)$ with $n_1^\pm \neq 0$ is written as

$$W_z(n_1) = P \exp \left[-ig \int_0^\infty d\lambda n_1 \cdot A(z + \lambda n_1) \right], \quad (29)$$

and the definition of the Wilson line $W_y(n_2)$ is similar. It is understood that the two Wilson lines $W_z(n_1)$ and $W_0(n_1)$ ($W_y(n_2)$ and $W_0(n_2)$) are connected by a vertical link at infinity [27, 28]. Equation (27) ((28)) produces additional light-cone singularities [25, 29, 30] from the region with a loop momentum collinear to n_- (n_+), as the Wilson line direction approaches the light cone, i.e., as $n_1 \rightarrow n_-$ ($n_2 \rightarrow n_+$) [29]. Hence, n_1^2 and n_2^2 serve as the infrared regulators for the light-cone singularities in our formalism. The B meson and pion wave functions then depend on the scales $\zeta_1^2 \equiv 4(n_1 \cdot P_1)^2 / |n_1^2|$ and $\zeta_2^2 \equiv 4(n_2 \cdot P_2)^2 / |n_2^2|$, respectively, whose variation is regarded as a factorization-scheme dependence. This scheme dependence, entering the hard kernel when taking the difference between the quark diagrams and the effective diagrams, can be minimized by adhering to fixed n_1^2 and n_2^2 .

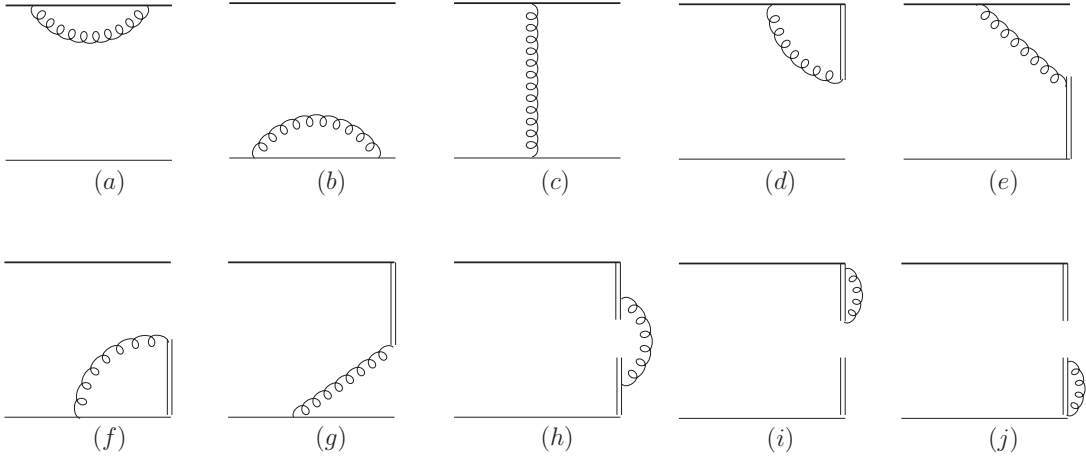


FIG. 5: $O(\alpha_s)$ diagrams for the B meson wave function.

We compute the convolution of the NLO wave function $\Phi_B^{(1)}$ with the LO hard kernel $H^{(0)}$ over the integration variables x'_1 and \mathbf{k}'_{1T} ,

$$\Phi_B^{(1)} \otimes H^{(0)} \equiv \int dx'_1 d^2 \mathbf{k}'_{1T} \Phi_B^{(1)}(x_1, \mathbf{k}_{1T}; x'_1, \mathbf{k}'_{1T}) H^{(0)}(x'_1, \mathbf{k}'_{1T}, x_2, \mathbf{k}_{2T}). \quad (30)$$

The sign of the plus component n_1^+ of the vector n_1 is arbitrary, which could be positive or negative (n_1^- has a positive sign, the same as of P_2^-). Choosing $n_1^+ < 0$, i.e., $n_1^2 < 0$ as in [1, 7, 31], we derive, from Figs. 5(a)-5(g),

$$\Phi_{5a}^{(1)} \otimes H^{(0)} = \frac{\alpha_s C_F}{4\pi} \left(\frac{1}{\epsilon} + \ln \frac{4\pi\mu_f^2}{m_g^2 e^{\gamma_E}} \right) H^{(0)}, \quad (31)$$

$$\Phi_{5b}^{(1)} \otimes H^{(0)} = -\frac{\alpha_s C_F}{8\pi} \left(\frac{1}{\epsilon} + \ln \frac{4\pi\mu_f^2}{\delta_1 m_B^2 e^{\gamma_E}} + 2 \right) H^{(0)}, \quad (32)$$

$$\Phi_{5c}^{(1)} \otimes H^{(0)} = -\frac{\alpha_s C_F}{4\pi} \left(\ln^2 \frac{\delta_1}{x_1^2} \right) H^{(0)}, \quad (33)$$

$$\Phi_{5d}^{(1)} \otimes H^{(0)} = -\frac{\alpha_s C_F}{4\pi} \ln \frac{\zeta_1^2}{m_B^2} \left(\frac{1}{\epsilon} + \ln \frac{4\pi\mu_f^2}{m_g^2 e^{\gamma_E}} \right) H^{(0)}, \quad (34)$$

$$\Phi_{5e}^{(1)} \otimes H^{(0)} = \frac{\alpha_s C_F}{4\pi} \ln \frac{\zeta_1^2}{m_B^2} \left(\ln \frac{\zeta_1^2}{m_g^2} + \frac{1}{2} \ln \frac{\zeta_1^2}{m_B^2} + 2 \ln x_1 \right) H^{(0)}, \quad (35)$$

$$\Phi_{5f}^{(1)} \otimes H^{(0)} = \frac{\alpha_s C_F}{4\pi} \left(\frac{1}{\epsilon} + \ln \frac{4\pi\mu_f^2}{x_1^2 \zeta_1^2 e^{\gamma_E}} - \ln^2 \frac{\delta_1 m_B^2}{x_1^2 \zeta_1^2} - 2 \ln \frac{\delta_1 m_B^2}{x_1^2 \zeta_1^2} + \frac{\pi^2}{3} \right) H^{(0)}, \quad (36)$$

$$\Phi_{5g}^{(1)} \otimes H^{(0)} = \frac{\alpha_s C_F}{4\pi} \left(\ln^2 \frac{\delta_1 m_B^2}{x_1^2 \zeta_1^2} - \frac{2\pi^2}{3} \right) H^{(0)}, \quad (37)$$

μ_f being the factorization scale. The two-particle reducible diagrams Figs. 5(a) and 5(c) are calculated, since the effective heavy-quark field employed in the B meson wave function differs from the b quark field in the quark diagrams. Though the effective diagrams and the quark diagrams have the same soft poles, the finite pieces are different, which contribute to the NLO hard kernel. The self-energy corrections to the Wilson lines in Figs. 5(h)-5(j) yield

$$\left(\Phi_{5h}^{(1)} + \Phi_{5i}^{(1)} + B_{5j}^{(1)} \right) \otimes H^{(0)} = \frac{\alpha_s C_F}{2\pi} \left(\frac{1}{\epsilon} + \ln \frac{4\pi\mu_f^2}{\delta_{12} m_B^2 e^{\gamma_E}} \right) H^{(0)}, \quad (38)$$

the same as in the pion wave function [13].

It is pointed out that the gluon mass m_g has been adopted to regularize the soft divergences in the diagrams involving the effective heavy-quark field, namely, Figs. 5(a), 5(d), and 5(e). The soft divergence in Fig. 5(a) indeed cancels that in Fig. 2(a) as stated in the previous subsection. The m_g dependence disappears in the sum of Eqs. (34)

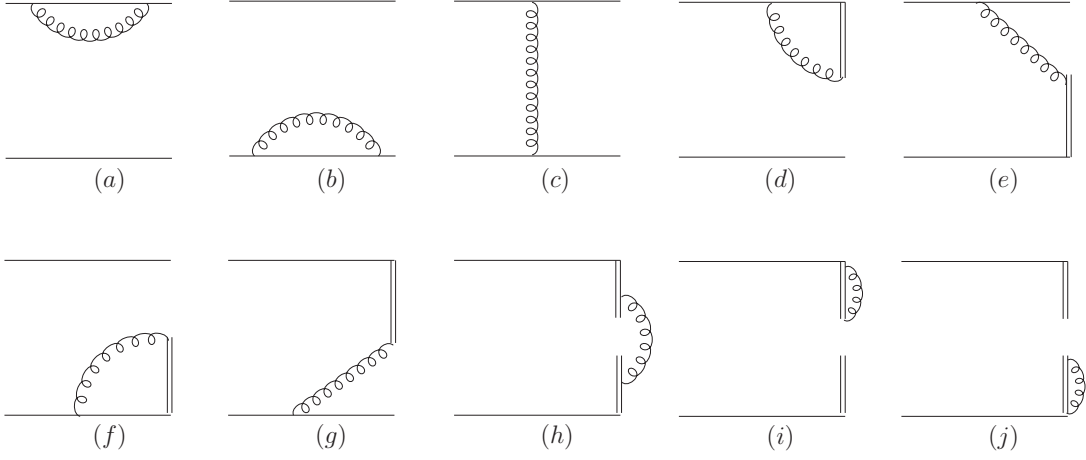


FIG. 6: $O(\alpha_s)$ diagrams for the pion wave function.

and (35), which must be the case, because the gluons emitted by the b quark and attaching to other particle lines do not generate soft divergences. The hierarchy $\zeta_1^2 \gg m_B^2$ was employed in the derivation of Eq. (35) [25], so the large double logarithm $\ln^2(\zeta_1^2/m_B^2)$ demands an additional resummation treatment of the B meson wave function, which will not be performed in this work. The double logarithms $\ln^2 \delta_1$ from the quark diagram Fig. 4(d) and from the effective diagram Fig. 5(c) cancel each other. The double logarithms $\ln^2(m_B^2 \delta_1 / (x_1^2 \zeta_1^2))$ are not only attenuated by x_1^2 , but also cancel exactly between Eqs. (36) and (37). Summing all the above $O(\alpha_s)$ contributions, we obtain

$$\begin{aligned} \Phi_B^{(1)} \otimes H^{(0)} &= \frac{\alpha_s C_F}{4\pi} \left[\left(\ln \frac{m_B^2}{\zeta_1^2} + \frac{7}{2} \right) \left(\frac{1}{\epsilon} + \ln \frac{4\pi\mu_f^2}{m_B^2 e^{\gamma_E}} \right) - \ln^2 \delta_1 + \left(4 \ln x_1 - \frac{3}{2} \right) \ln \delta_1 + \ln \frac{m_B^2}{m_g^2} \right. \\ &\quad \left. + \frac{3}{2} \ln^2 \frac{m_B^2}{\zeta_1^2} - (2 \ln x_1 - 1) \ln \frac{m_B^2}{\zeta_1^2} - 4 \ln^2 x_1 - 2 \ln(x_2 \eta) - \frac{\pi^2}{3} - 1 \right] H^{(0)}. \end{aligned} \quad (39)$$

We then compute the convolution of the NLO wave function $\Phi_\pi^{(1)}$ with the LO hard kernel $H^{(0)}$ over the integration variables x'_2 and \mathbf{k}'_{2T} ,

$$H^{(0)} \otimes \Phi_\pi^{(1)} \equiv \int dx'_2 d^2 \mathbf{k}'_{2T} H^{(0)}(x_1, \mathbf{k}_{1T}, x'_2, \mathbf{k}'_{2T}) \Phi_\pi^{(1)}(x_2, \mathbf{k}_{2T}; x'_2, \mathbf{k}'_{2T}). \quad (40)$$

The corrections from Figs. 6(a)-6(j) are summarized as

$$H^{(0)} \otimes \Phi_{6a}^{(1)} = H^{(0)} \otimes \Phi_{6b}^{(1)} = -\frac{\alpha_s C_F}{8\pi} \left(\frac{1}{\epsilon} + \ln \frac{4\pi\mu_f^2}{\delta_2 m_B^2 e^{\gamma_E}} + 2 \right) H^{(0)}, \quad (41)$$

$$H^{(0)} \otimes \Phi_{6c}^{(1)} = 0, \quad (42)$$

$$H^{(0)} \otimes \Phi_{6d}^{(1)} = \frac{\alpha_s C_F}{4\pi} \left(\frac{1}{\epsilon} + \ln \frac{4\pi\mu_f^2}{\delta_2 m_B^2 e^{\gamma_E}} - \ln^2 \frac{\zeta_2^2}{\delta_2 m_B^2} + \ln \frac{\zeta_2^2}{\delta_2 m_B^2} + 2 - \frac{\pi^2}{3} \right) H^{(0)}, \quad (43)$$

$$H^{(0)} \otimes \Phi_{6e}^{(1)} = \frac{\alpha_s C_F}{4\pi} \left(\ln^2 \frac{x_2 \zeta_2^2}{\delta_2 m_B^2} + \pi^2 \right) H^{(0)}, \quad (44)$$

$$H_b^{(0)} \otimes \Phi_{6f}^{(1)} = \frac{\alpha_s C_F}{4\pi} \left(\frac{1}{\epsilon} + \ln \frac{4\pi\mu_f^2}{\delta_2 m_B^2 e^{\gamma_E}} - \ln^2 \frac{x_2^2 \zeta_2^2}{\delta_2 m_B^2} + \ln \frac{x_2^2 \zeta_2^2}{\delta_2 m_B^2} + 2 - \frac{\pi^2}{3} \right) H^{(0)}, \quad (45)$$

$$H^{(0)} \otimes \Phi_{6g}^{(1)} = \frac{\alpha_s C_F}{4\pi} \left(\ln^2 \frac{\delta_2 m_B^2}{x_2^2 \zeta_2^2} - \frac{\pi^2}{3} \right) H^{(0)}, \quad (46)$$

$$H^{(0)} \otimes \left(\Phi_{6h}^{(1)} + \Phi_{6i}^{(1)} + \Phi_{6j}^{(1)} \right) = \frac{\alpha_s C_F}{2\pi} \left(\frac{1}{\epsilon} + \ln \frac{4\pi\mu_f^2}{\delta_{12} m_B^2 e^{\gamma_E}} \right) H^{(0)}, \quad (47)$$

which are similar to those extracted from the pion transition and electromagnetic form factors [13, 15], but with the hard scale Q being replaced by m_B here. This similarity supports the universality of the pion wave function.

Summing all the above $O(\alpha_s)$ contributions, we have

$$H^{(0)} \otimes \Phi_\pi^{(1)} = \frac{\alpha_s C_F}{4\pi} \left[3 \left(\frac{1}{\epsilon} + \ln \frac{4\pi\mu_f^2}{m_B^2 e^{\gamma_E}} \right) - \ln \delta_2 (2 \ln x_2 + 3) + 2 \ln \frac{\zeta_2^2}{m_B^2} (\ln x_2 + 1) - 2 \ln \delta_{12} + \ln x_2 (\ln x_2 + 2) + 2 \right] H^{(0)}. \quad (48)$$

We stress that the ultraviolet poles are different in Eqs. (39) and (48), since the former involves the effective heavy-quark field, instead of the b quark field. That is, the B meson and pion wave functions exhibit different evolutions as illustrated below. First, the B meson decay constant, defined via the matrix element with the effective heavy-quark field, evolves with an energy scale. Hence, part of the $\ln \mu_f$ term in Eq. (39) should be absorbed into $f_B(\mu_f)$ through the RG equation in the heavy quark effective theory (HQET)

$$\left(\mu \frac{d}{d\mu} + \frac{\alpha_s C_F}{4\pi} \gamma_f \right) f_B(\mu_f) = 0, \quad (49)$$

with the anomalous dimension $\gamma_f = -3$ at one loop [32]. The RG equation for the B meson wave function without the decay constant, $\Phi_B(x_1, \mu_f)/f_B(\mu_f)$, is then written as

$$\left(\mu \frac{d}{d\mu} + \frac{\alpha_s C_F}{4\pi} \gamma_B \right) \frac{\Phi_B(x_1, \mu_f)}{f_B(\mu_f)} = 0, \quad (50)$$

where the anomalous dimension

$$\gamma_B = -2 \left(\ln \frac{m_B^2}{\zeta_1^2} + 2 \right), \quad (51)$$

governs part of the RG evolution in the k_T factorization formulas for the $B \rightarrow \pi$ form factors [1, 21].

C. NLO Hard Kernel

The infrared-finite k_T -dependent NLO hard kernel for the $B \rightarrow \pi$ transition form factors is derived by taking the difference between the quark diagrams and the effective diagrams [14]

$$\begin{aligned} H^{(1)}(x_1, \mathbf{k}_{1T}, x_2, \mathbf{k}_{2T}) &= G^{(1)}(x_1, \mathbf{k}_{1T}, x_2, \mathbf{k}_{2T}) \\ &\quad - \int dx'_1 d^2 \mathbf{k}'_{1T} \Phi_B^{(1)}(x_1, \mathbf{k}_{1T}; x'_1, \mathbf{k}'_{1T}) H^{(0)}(x'_1, \mathbf{k}'_{1T}, x_2, \mathbf{k}_{2T}) \\ &\quad - \int dx'_2 d^2 \mathbf{k}'_{2T} H^{(0)}(x_1, \mathbf{k}_{1T}, x'_2, \mathbf{k}'_{2T}) \Phi_\pi^{(1)}(x_2, \mathbf{k}_{2T}; x'_2, \mathbf{k}'_{2T}). \end{aligned} \quad (52)$$

Note that α_s appearing in Eqs. (26), (39), and (48) denotes the bare coupling constant, which can be rewritten as

$$\alpha_s = \alpha_s(\mu_f) + \delta Z(\mu_f) \alpha_s(\mu_f), \quad (53)$$

with the counterterm δZ being defined in the modified minimal subtraction scheme. We insert Eq. (53) into the expressions of the LO and NLO quark diagrams, and of the NLO effective diagrams. The LO hard kernel $H^{(0)}$ multiplied by δZ then regularizes the ultraviolet pole in Eq. (26). The ultraviolet poles in Eqs. (39) and (48) are regularized by the counterterm of the quark field and by an additive counterterm in the modified minimal subtraction scheme.

The NLO hard kernel for Fig. 1(a) is given by

$$\begin{aligned} H^{(1)} &= \frac{\alpha_s(\mu_f) C_F}{4\pi} \left[\frac{21}{4} \ln \frac{\mu^2}{m_B^2} - \left(\ln \frac{m_B^2}{\zeta_1^2} + \frac{13}{2} \right) \ln \frac{\mu_f^2}{m_B^2} + \frac{9}{16} (\ln^2 x_1 + 2 \ln x_1 \ln x_2 - \ln x_2^2) \right. \\ &\quad + \left(2 \ln \frac{m_B^2}{\zeta_1^2} + \frac{7}{8} \ln \eta - \frac{1}{4} \right) \ln x_1 + \left(2 \ln \frac{m_B^2}{\zeta_2^2} + \frac{7}{8} \ln \eta - \frac{5}{2} \right) \ln x_2 + 2 \ln \frac{m_B^2}{\zeta_2^2} + \left(\frac{15}{4} - \frac{7}{16} \ln \eta \right) \ln \eta \\ &\quad \left. - \frac{1}{2} \ln \frac{m_B^2}{\zeta_1^2} \left(3 \ln \frac{m_B^2}{\zeta_1^2} + 2 \right) + \frac{85}{48} \pi^2 + \frac{219}{16} \right] H^{(0)}, \end{aligned} \quad (54)$$

in which all the infrared regulators m_g , δ_1 , and δ_2 have disappeared. A choice of the scales ζ_1 and ζ_2 corresponds to a factorization scheme, which should be fixed for consistency. Following the scheme $\zeta^2 = Q^2$ adopted in the NLO analysis of the pion transition and electromagnetic form factors [13, 15], we set ζ_2 to m_B^2 . The important logarithms $\ln(m_B^2/\zeta_1^2)$, arising from the B meson wave function, enter the hard kernel after the infrared subtraction. Instead of performing resummation of these logarithms, we choose a sufficiently large ζ_1 , say, $\zeta_1/m_B = 25$ in the numerical analysis, which has been assumed for achieving the simplified result in Eq. (35). In this scheme the $\ln^2(m_B/\zeta_1)$ term happens to cancel the large constant term in the hard kernel, and reduces the NLO correction.

Moreover, the double logarithm $\ln^2 x_2$ has been absorbed into the jet function $J(x_2)$ [22] defined in the kinematic region where the virtual b quark in Fig. 1(a) becomes almost on-shell, namely, with $x_2 \rightarrow 0$. The organization of this important logarithm to all orders leads to the threshold resummation factor, which further suppresses the end-point singularity from small x_2 in the $B \rightarrow \pi$ form factors [21]. Therefore, we have to subtract the NLO jet function [15]

$$J^{(1)}H^{(0)} = -\frac{\alpha_s}{4\pi}C_F \left(\ln^2 x_2 + \ln x_2 + \frac{\pi^2}{3} \right) H^{(0)}, \quad (55)$$

from Eq. (54), which finally turns into

$$\begin{aligned} H^{(1)} &\rightarrow H^{(1)} - J^{(1)}H^{(0)} \\ &= \frac{\alpha_s(\mu_f)C_F}{4\pi} \left[\frac{21}{4} \ln \frac{\mu^2}{m_B^2} - \left(\ln \frac{m_B^2}{\zeta_1^2} + \frac{13}{2} \right) \ln \frac{\mu_f^2}{m_B^2} + \frac{7}{16} \ln^2(x_1 x_2) + \frac{1}{8} \ln^2 x_1 + \frac{1}{4} \ln x_1 \ln x_2 \right. \\ &\quad + \left(2 \ln \frac{m_B^2}{\zeta_1^2} + \frac{7}{8} \ln \eta - \frac{1}{4} \right) \ln x_1 + \left(\frac{7}{8} \ln \eta - \frac{3}{2} \right) \ln x_2 + \left(\frac{15}{4} - \frac{7}{16} \ln \eta \right) \ln \eta \\ &\quad \left. - \frac{1}{2} \ln \frac{m_B^2}{\zeta_1^2} \left(3 \ln \frac{m_B^2}{\zeta_1^2} + 2 \right) + \frac{101}{48} \pi^2 + \frac{219}{16} \right] H^{(0)}. \end{aligned} \quad (56)$$

Because the double logarithm $\ln^2 x_1$ was not resummed in [21], it is left in the above NLO hard kernel $H^{(1)}$. Another double logarithm $\ln^2(x_1 x_2)$ actually arises from the approximation $\ln^2 \delta_{12} \approx \ln^2(x_1 x_2)$. This approximation makes sense: a logarithm does not develop an end-point singularity, so the k_T^2 term is negligible in $\ln \delta_{12}$. Equation (56), proportional to P_2^μ , generates the NLO corrections at leading twist to the $B \rightarrow \pi$ transition form factors $f^+(q^2)$ and $f^0(q^2)$ in Eq. (1).

III. NUMERICAL ANALYSIS

In this section we evaluate the $B \rightarrow \pi$ transition form factors numerically in the k_T factorization up to NLO, adopting the following non-asymptotic pion distribution amplitudes [33, 34],

$$\begin{aligned} \phi_\pi^A(x) &= \frac{6f_\pi}{2\sqrt{2}N_c} x(1-x) \left[1 + a_2 C_2^{3/2}(u) + a_4 C_4^{3/2}(u) \right], \\ \phi_\pi^P(x) &= \frac{f_\pi}{2\sqrt{2}N_c} \left[1 + 0.59 C_2^{1/2}(u) + 0.09 C_4^{1/2}(u) \right], \\ \phi_\pi^\sigma(x) &= \frac{6f_\pi}{2\sqrt{2}N_c} x(1-x) \left[1 + 0.11 C_2^{3/2}(u) \right], \end{aligned} \quad (57)$$

with the pion decay constant $f_\pi = 130$ MeV, the Gegenbauer moments $a_2 = 0.16$ and $a_4 = 0.04$, and the Gegenbauer polynomials

$$\begin{aligned} C_1^{1/2}(u) &= u, & C_1^{3/2}(u) &= 3u, \\ C_2^{1/2}(u) &= \frac{1}{2}(3u^2 - 1), & C_2^{3/2}(u) &= \frac{3}{2}(5u^2 - 1), \\ C_3^{1/2}(u) &= \frac{1}{2}u(5u^2 - 3), & C_4^{3/2}(u) &= \frac{15}{8}(21u^4 - 14u^2 + 1), \end{aligned} \quad (58)$$

and the variable $u = 1 - 2x$. The B meson distribution amplitudes inspired from a QCD sum rule analysis in the HQET [35]

$$\begin{aligned} \phi_B^{(+)}(x, b) &= \frac{f_B}{2\sqrt{2}N_c} x \left(\frac{m_B}{\omega_0} \right)^2 \text{Exp} \left[-\frac{xm_B}{\omega_0} - \frac{1}{2}(\omega_0 b)^2 \right], \\ \phi_B^{(-)}(x, b) &= \frac{f_B}{2\sqrt{2}N_c} \left(\frac{m_B}{\omega_0} \right) \text{Exp} \left[-\frac{xm_B}{\omega_0} - \frac{1}{2}(\omega_0 b)^2 \right], \end{aligned} \quad (59)$$

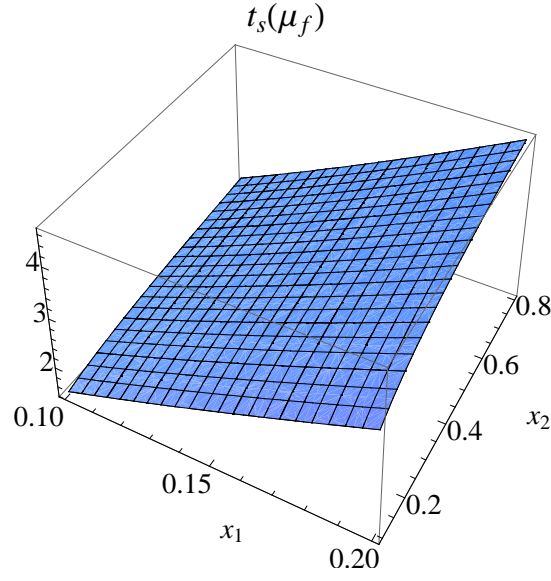


FIG. 7: Renormalization scale $t_s(\mu_f)$, defined in Eq. (61), as a function of momentum fractions x_1 and x_2 for a typical factorization scale $\mu_f = 1.5$ GeV and the ratio $\zeta_1/m_B = 25$.

are employed, where the B meson decay constant is set to a constant $f_B = 214$ MeV for convenience (namely, neglecting its evolution), and the shape parameter is chosen as $\omega_0 = 0.35$ GeV.

The first issue concerns the choice of the renormalization scale μ and the factorization scale μ_f in order to minimize the NLO corrections to the form factors. For the first choice, μ_f is set to the hard scales specified in the PQCD approach to exclusive processes [2, 7, 36]

$$t^a = \max(\sqrt{x_2\eta} m_B, 1/b_1, 1/b_2), \quad t^b = \max(\sqrt{x_1\eta} m_B, 1/b_1, 1/b_2), \quad (60)$$

corresponding to the largest energy scales in Figs. 1(a) and 1(b), respectively. Then we utilize the freedom of choosing μ to diminish all the single-logarithmic and constant terms in the NLO hard kernel, which is found to be

$$t_s(\mu_f) = \left\{ \text{Exp} \left[c_1 + \left(\ln \frac{m_B^2}{\zeta_1^2} + \frac{5}{4} \right) \ln \frac{\mu_f^2}{m_B^2} \right] x_1^{c_2} x_2^{c_3} \right\}^{2/21} \mu_f, \quad (61)$$

with the coefficients

$$\begin{aligned} c_1 &= - \left(\frac{15}{4} - \frac{7}{16} \ln \eta \right) \ln \eta + \frac{1}{2} \ln \frac{m_B^2}{\zeta_1^2} \left(3 \ln \frac{m_B^2}{\zeta_1^2} + 2 \right) - \frac{101}{48} \pi^2 - \frac{219}{16}, \\ c_2 &= - \left(2 \ln \frac{m_B^2}{\zeta_1^2} + \frac{7}{8} \ln \eta - \frac{1}{4} \right), \\ c_3 &= - \frac{7}{8} \ln \eta + \frac{3}{2}. \end{aligned}$$

To have an idea of the magnitude of the renormalization scale $\mu = t_s(\mu_f)$, we display its behavior in the dominant region with the small momentum fractions x_1 and x_2 in Fig. 7, where the factorization scale μ_f is fixed at its typical value 1.5 GeV. The ratio of the NLO contributions over the total ones as a function of the transfer momentum squared q^2 is summarized in Fig. 8, which is approximately 30% for both the form factors $f^+(q^2)$ and $f^0(q^2)$. In the second choice, we set both scales to $\mu = \mu_f = t^a$ (t^b) in the factorization formula associated with Fig. 1(a) (1(b)). It turns out that this simple scenario yields larger NLO corrections around 40% as shown in Fig. 8. The third choice corresponds to $\mu_f = m_B$ and $\mu = t_s(\mu_f)$, for which the NLO corrections are approximately 15%. However, the inverse relation $\mu_f > \mu$ in this case seems not to be natural. Hereafter, we shall adopt the first choice of the renormalization and factorization scales as the default one.

The $B \rightarrow \pi$ transition form factors in the k_T factorization up to NLO are presented in Fig. 9. It is observed that the LO and NLO contributions exhibit the similar power-law behavior, as they should. It is not a surprise that the

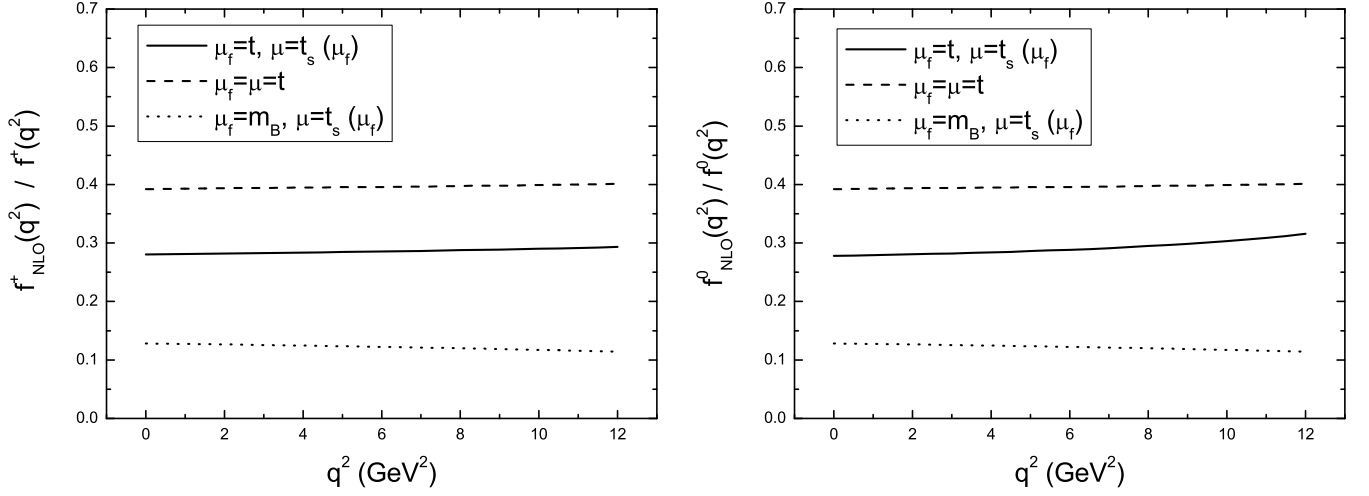


FIG. 8: Ratios of the NLO corrections over the total contributions to the $B \rightarrow \pi$ form factors for three different choices of the renormalization and factorization scales.

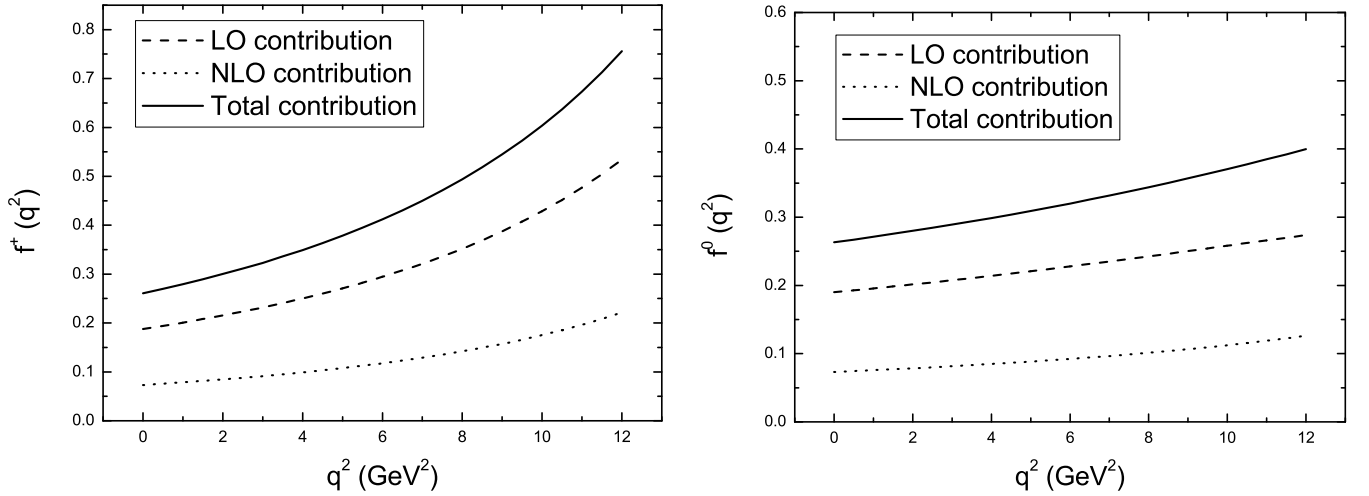


FIG. 9: LO and NLO contributions to the $B \rightarrow \pi$ form factors with the non-asymptotic pion distribution amplitudes in Eq. (57) and the first scenario for the scale choice, $\mu_f = t$ and $\mu = t_s(\mu_f)$.

form factors at the maximal recoil of the pion, $f^+(0) = f^0(0)$, are close to their LO value [21], even after including the NLO contributions. The reason is that the meson wave functions have been adjusted accordingly to maintain this value, which is regarded as an input. That is, when choosing hadron wave functions in the PQCD approach, one must pay attention to the order in the coupling constant, at which the hadron wave functions are determined. Though the form-factor values, treated as inputs, are not changed at higher orders, the different hadron wave functions extracted at different orders do affect other topologies of nonleptonic two-body B meson decay amplitudes. It is worthwhile to investigate the corrections to nonleptonic two-body B meson decays from this NLO source in future works.

To test the impact of higher conformal-spin partial waves in the pion distribution amplitudes, we plot the q^2 dependence of the form factors in Fig. 10 with the asymptotic pion distribution amplitudes. Numerically, both the form factors are reduced by about 25% for $q^2 \leq 12 \text{ GeV}^2$ without the non-asymptotic Gegenbauer terms in Eq. (57). We also investigate the effects from different models of the B meson distribution amplitudes. A model widely adopted in the PQCD analysis is given by

$$\phi_B^{(+)}(x, b) = \phi_B^{(-)}(x, b) = \frac{f_B}{2\sqrt{2}N_c} N_B x^2(1-x)^2 \text{Exp} \left[-\frac{x^2 m_B}{2\omega_0^2} - \frac{1}{2}(\omega_0 b)^2 \right], \quad (62)$$

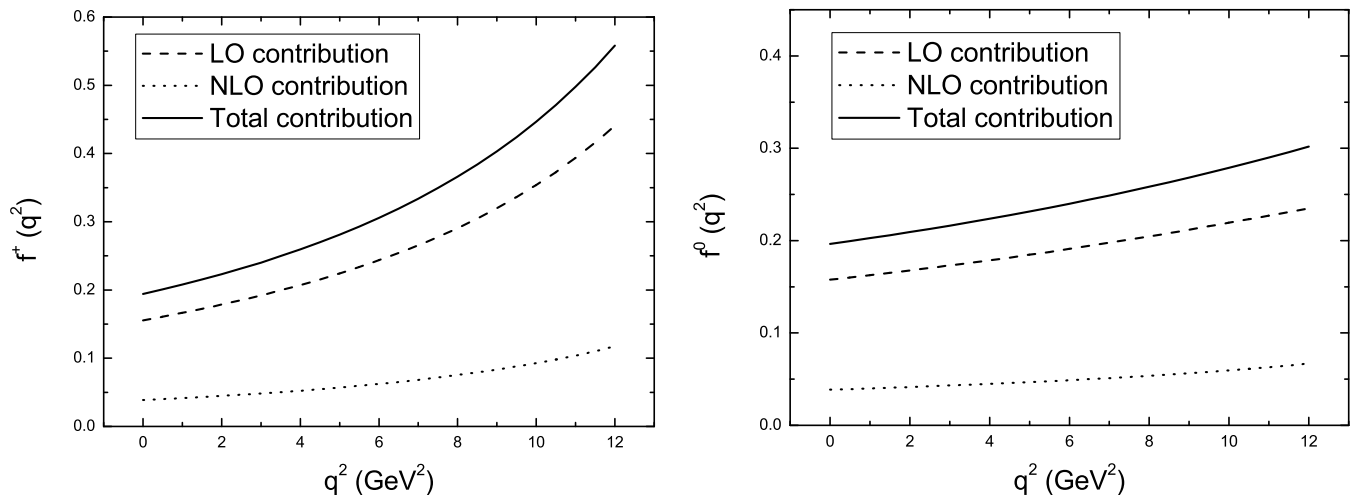


FIG. 10: LO and NLO contributions to the $B \rightarrow \pi$ form factors with the asymptotic pion distribution amplitudes and the first scenario for the scale choice, $\mu_f = t$ and $\mu = t_s(\mu_f)$.

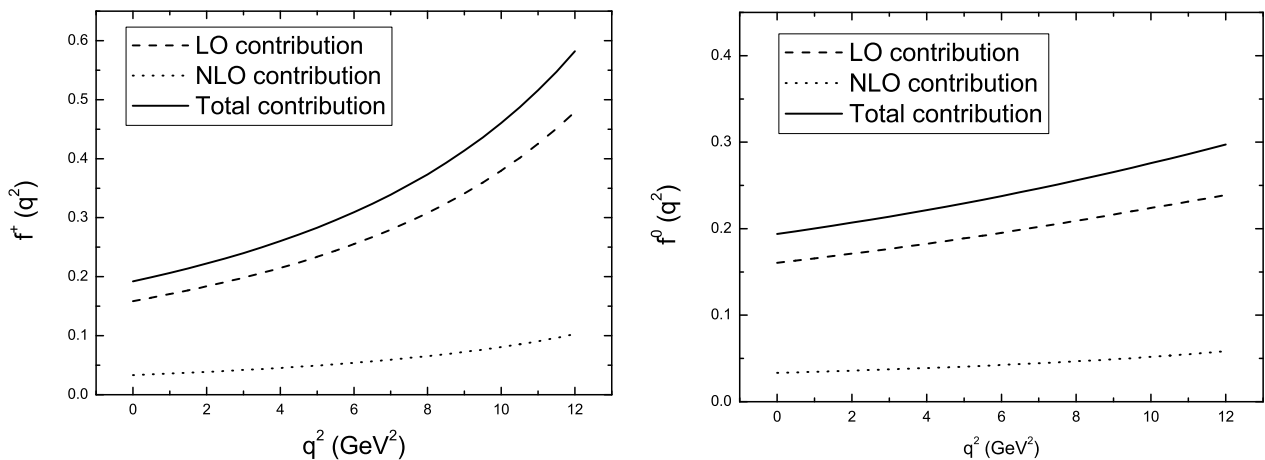


FIG. 11: LO and NLO contributions to the $B \rightarrow \pi$ form factors with the B meson distribution amplitudes in Eq. (62) and the first scenario for the scale choice: $\mu_f = t$ and $\mu = t_s(\mu_f)$.

with the normalization constant N_B defined via $\int dx \phi_B^{(+)}(x, 0) = f_B / (2\sqrt{2N_c})$. Note that the two leading B meson distribution amplitudes have been assumed to be equal for the purpose of numerical estimate, which do not obey the equations of motion [37]. Besides, it exhibits an asymptotic behavior at $x \rightarrow 0$ different from that derived in [38]. The corresponding q^2 dependence in Fig. 11 indicates that the form factors with the model in Eq. (62) are approximately 25% smaller than those with the model in Eq. (59). It is interesting to notice in Fig. 11 that the NLO corrections are relatively small, less than 20% of the total contributions. The reason is attributed to the fact that the end-point region of x_1 is strongly suppressed by this model and the double logarithm $\ln^2 x_1$ in the NLO hard kernel does not play an essential role.

The extraction of the Cabibbo-Kobayashi-Maskawa matrix element $|V_{ub}|$ [39] from the semileptonic decay $B \rightarrow \pi \ell \bar{\nu}$ is of intensive phenomenological interest recently (see [34] and references therein). Here we comment on the consistency of the $B \rightarrow \pi$ form factors predicted in the NLO k_T factorization with those in the literature, in view of the extraction of $|V_{ub}|$. For this purpose, we also estimate the theoretical uncertainties of the form factors $f^+(q^2)$ and $f^0(q^2)$ from the variations of the Gegenbauer moments a_2 and a_4 in the twist-2 pion distribution amplitudes, from the variations of the chiral scale $m_0 \equiv m_\pi^2 / (m_u + m_d)$, m_u (m_d) being the u (d) quark mass, involved in the two-parton twist-3 pion distribution amplitudes [40], and from the variations of the shape parameter ω_0 in the B meson distribution amplitudes in Eq. (59). Unfortunately, the extraction of ω_0 still suffers large uncertainty from QCD sum-rule calculations. We

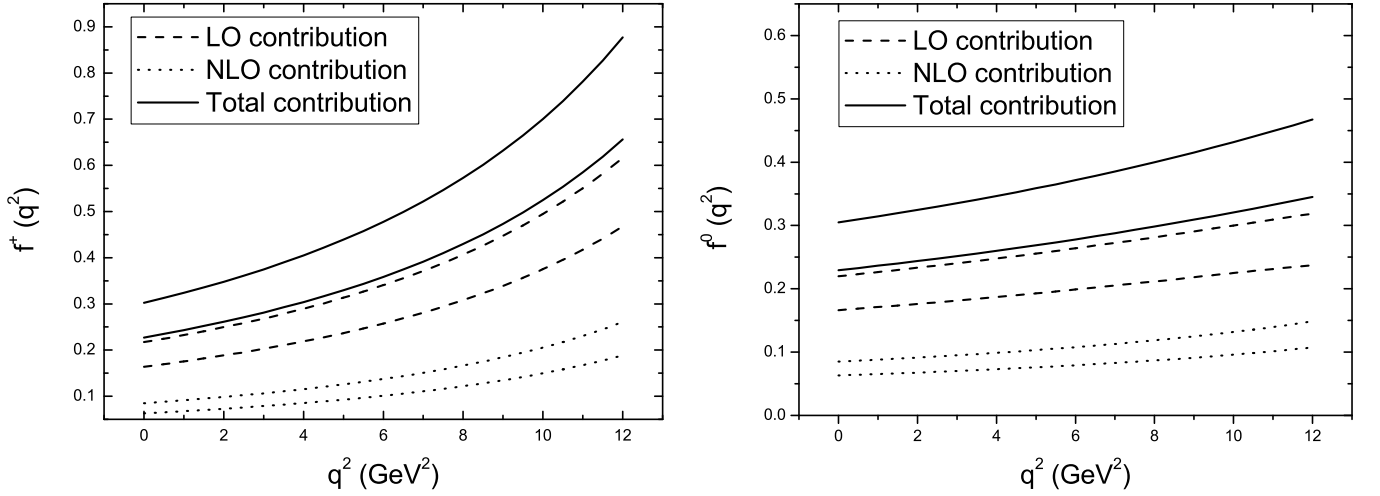


FIG. 12: LO and NLO contributions to the $B \rightarrow \pi$ form factors with the B meson distribution amplitudes in Eq. (59), however, varying the shape parameter ω_0 from 0.30 GeV to 0.40 GeV and the first scenario for the scale choice: $\mu_f = t$ and $\mu = t_s(\mu_f)$.

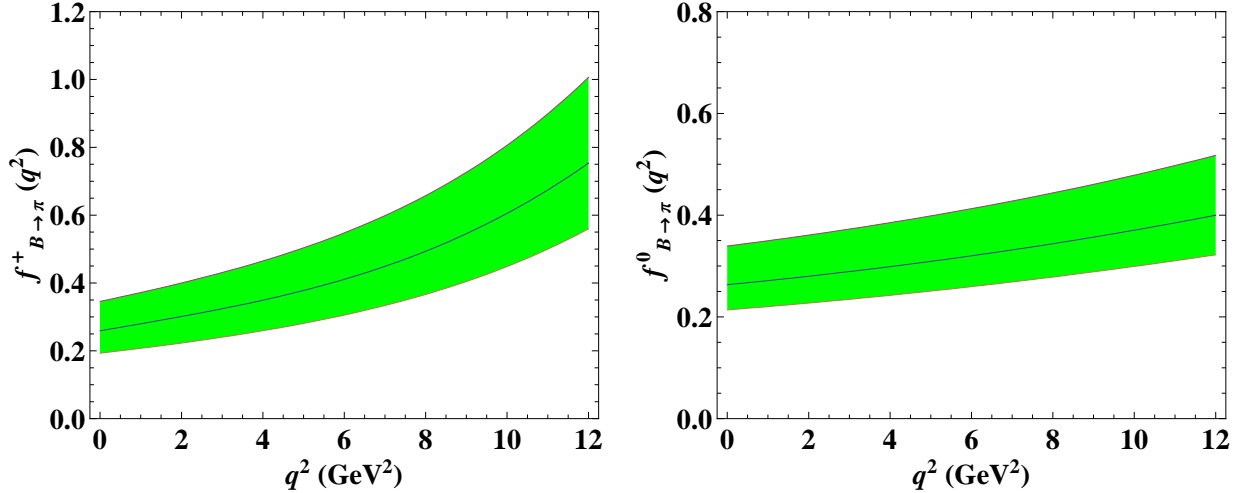


FIG. 13: Theoretical uncertainties of the $B \rightarrow \pi$ form factors with the first scenario for the scale choice: $\mu_f = t$ and $\mu = t_s(\mu_f)$.

simply take $\omega_0 = 0.35 \pm 0.05$ GeV to illustrate the effect on the form factors from the variation of ω_0 . It is seen from Fig. 12 that both the form factors $f^+(q^2)$ and $f^0(q^2)$, including LO and NLO contributions, increase (decrease) by 15 % with the decrease (increase) of ω_0 . Combining the uncertainties due to $a_2(1\text{GeV}) = 0.16^{+0.09}_{-0.07}$, $a_4(1\text{GeV}) = 0.04^{+0.12}_{-0.08}$, $m_0(1\text{GeV}) = 1.74^{+0.67}_{-0.38}$ GeV, and $\omega_0 = 0.35 \pm 0.05$ GeV, we predict the form factors $f^+(q^2)$ and $f^0(q^2)$ as displayed in Fig. 13. Fitting to the BaBar data on the integrated $B \rightarrow \pi \ell \bar{\nu}$ branching ratio within the region $0 \leq q^2 \leq 8$ GeV² [41], where the leading-twist k_T factorization is expected to work well, we obtain

$$|V_{ub}| = 2.90^{+0.77}_{-0.80} \Big|_{th.} \Big|_{-0.14}^{+0.13} \Big|_{exp.} \quad (63)$$

The above value is in good agreement with that in [41], which employed the data on q^2 bins in the whole kinematic region and the lattice QCD results of the $B \rightarrow \pi$ form factors from the FNAL/MILC Collaboration [42]. Equation (63), however, differs from $|V_{ub}| = 3.59^{+0.38}_{-0.33} \Big|_{th.} \pm 0.11 \Big|_{exp.}$ extracted in [34], where the $B \rightarrow \pi$ form factors were computed in the light-cone sum rule (LCSR). The distinction can be traced back to the different q^2 dependence of the form factor $f^+(q^2)$ predicted in the k_T factorization and in LCSR, albeit with the similar $f^+(0)$ value in both approaches. More dedicated efforts on the study of the shape of $B \rightarrow \pi$ form factors in QCD is in demand in order to resolve the potential difference in the extraction of $|V_{ub}|$.

IV. CONCLUSION

In this paper we have calculated the NLO corrections to the $B \rightarrow \pi$ transition form factors at leading twist in the k_T factorization theorem. Both the collinear and soft divergences in the NLO quark diagrams and in the NLO effective diagrams for meson wave functions are regularized by the off-shellness k_T^2 of light partons. The b quark remains on-shell, such that it can be approximated by the standard effective heavy quark in the k_T factorization. The key is that the soft gluons radiated by the b quark and attaching to other particle lines can be regularized by the virtuality of other particle lines. The NLO pion wave function is the same as constructed in the pion transition and electromagnetic form factors, confirming its universality. Compared to the pion wave function, the NLO B meson wave function contains the additional double logarithm $\ln^2(\zeta_1^2/m_B^2)$. Because of the assumed hierarchy $\zeta_1^2 \gg m_B^2$, the appearance of this double logarithm demands the implementation of the resummation technique, which is expected to minimize the scheme dependence from different choices of ζ_1 . This subject, together with the asymptotic behavior of the B meson wave function in the k_T factorization, will be discussed in a forthcoming work.

The exact cancellation of the infrared divergences between the quark diagrams and the effective diagrams verifies the validity of the k_T factorization for the B meson semileptonic decays at NLO level. Though the NLO hard kernel for the $B \rightarrow \pi$ transition form factors contains a huge constant term, it is reduced by the large double logarithm $\ln^2(\zeta_1^2/m_B^2)$ mentioned above. This is the reason why the conventional choice of the factorization scale in the PQCD approach, as the virtuality of internal particles, can work to render the NLO corrections under control. By tuning the renormalization scale to cancel the single-logarithmic and constant terms, which is still lower than the B meson mass in the dominant kinematic region, the NLO corrections are about 30% of the form factors. The effect of varying the meson wave functions has been also investigated: the model for the B meson wave function with a stronger suppression at a small momentum fraction, and the asymptotic model for the pion wave function lower the NLO corrections down to 20%.

Acknowledgement

We are grateful to Thomas Mannel for helpful discussions. The work was supported in part by the National Science Council of R.O.C. under Grant No. NSC-98-2112-M-001-015-MY3, by the National Center for Theoretical Sciences of R.O.C., by National Science Foundation of China under Grant No. 11005100, by the German research foundation DFG under contract MA1187/10-1, and by the German Ministry of Research (BMBF) under contract 05H09PSF.

-
- [1] H.-n. Li and H.-L. Yu, Phys. Rev. Lett. **74**, 4388 (1995); Phys. Lett. B **353**, 301 (1995); Phys. Rev. D **53**, 2480 (1996).
 - [2] Y.Y. Keum, H.-n. Li, and A.I. Sanda, Phys. Lett. B **504**, 6 (2001); Phys. Rev. D **63**, 054008 (2001); Y.Y. Keum and H.-n. Li, Phys. Rev. D **63**, 074006 (2001); C.-D. Lü, K. Ukai and M.-Z. Yang, Phys. Rev. D **63**, 074009 (2001).
 - [3] S. Catani, M. Ciafaloni and F. Hautmann, Phys. Lett. B **242**, 97 (1990); Nucl. Phys. B **366**, 135 (1991).
 - [4] J.C. Collins and R.K. Ellis, Nucl. Phys. B **360**, 3 (1991).
 - [5] E.M. Levin, M.G. Ryskin, Yu.M. Shabelskii, and A.G. Shuvaev, Sov. J. Nucl. Phys. **53**, 657 (1991).
 - [6] J. Botts and G. Sterman, Nucl. Phys. B **225**, 62 (1989).
 - [7] H.-n. Li and G. Sterman, Nucl. Phys. B **381**, 129 (1992).
 - [8] T. Huang and Q.-X. Shen, Z. Phys. C **50**, 139 (1991); J.P. Ralston and B. Pire, Phys. Rev. Lett. **65**, 2343 (1990); R. Jakob and P. Kroll, Phys. Lett. B **315**, 463 (1993); B **319**, 545 (1993)(E).
 - [9] H.-n. Li, S. Mishima, and A.I. Sanda, Phys. Rev. D **72**, 114005 (2005).
 - [10] H.-n. Li and S. Mishima, Phys. Rev. D **73**, 114014 (2006).
 - [11] H.-n. Li and S. Mishima, Phys. Rev. D **74**, 094020 (2006).
 - [12] H.-n. Li and S. Mishima, Phys. Rev. D **83**, 034023 (2011).
 - [13] H.-n. Li, Y.-L. Shen, Y.-M. Wang, and H. Zou, Phys. Rev. D **83**, 054029 (2011).
 - [14] M. Nagashima and H.-n. Li, Phys. Rev. D **67**, 034001 (2003).
 - [15] S. Nandi and H.-n. Li, Phys. Rev. D **76**, 034008 (2007).
 - [16] M. Beneke and Th. Feldmann, Nucl. Phys. **B592**, 3 (2001).
 - [17] C. W. Bauer, D. Pirjol and I. W. Stewart, Phys. Rev. D **67**, 071502 (2003).
 - [18] G.P. Lepage and S.J. Brodsky, Phys. Rev. D **22**, 2157 (1980).
 - [19] M. Beneke and Th. Feldmann, Nucl. Phys. B **685**, 249 (2004).
 - [20] A.V. Manohar and I.W. Stewart, Phys. Rev. D **76**, 074002 (2007).
 - [21] T. Kurimoto, H.-n. Li, and A.I. Sanda, Phys. Rev. D **65**, 014007 (2002).
 - [22] H.-n. Li, Phys. Rev. D **66**, 094010 (2002); K. Ukai and H.-n. Li, Phys. Lett. B **555**, 197 (2003).
 - [23] T. Huang and X.-G. Wu, Phys. Rev. D **71**, 034018 (2005).

- [24] W. Siegel, Phys. Lett. B **84**, 193 (1979).
- [25] H.-n. Li and H. S. Liao, Phys. Rev. D **70**, 074030 (2004).
- [26] H.-n. Li, Phys. Rev. D **64**, 014019 (2001); M. Nagashima and H.-n. Li, Eur. Phys. J. C **40**, 395 (2005).
- [27] X. Ji, and F. Yuan, Phys. Lett. B **543**, 66 (2002); A.V. Belitsky, X. Ji, and F. Yuan, Nucl. Phys. B **656**, 165 (2003).
- [28] I. O. Cherednikov and N. G. Stefanis, Nucl. Phys. B **802**, 146 (2008).
- [29] J.C. Collins, Acta. Phys. Polon. B **34**, 3103 (2003).
- [30] J.-P. Ma and Q. Wang, JHEP **0601**, 067 (2006); Phys. Lett. B **642**, 232 (2006).
- [31] H.-n. Li, Phys. Rev. D **55**, 105 (1997).
- [32] M. A. Shifman and M. B. Voloshin, Sov. J. Nucl. Phys. **45**, 292 (1987) [Yad. Fiz. **45**, 463 (1987)]. H. D. Politzer and M. B. Wise, Phys. Lett. B **206**, 681 (1988); Phys. Lett. B **208**, 504 (1988).
- [33] G. Duplancic, A. Khodjamirian, Th. Mannel, B. Melic, and N. Offen, JHEP **0804**, 014 (2008).
- [34] A. Khodjamirian, Th. Mannel, N. Offen and Y.-M. Wang, Phys. Rev. D **83**, 094031 (2011).
- [35] A.G. Grozin and M. Neubert, Phys. Rev. D **55**, 272 (1997).
- [36] C.-H. Chou, H.-H. Shih, S.-C. Lee and H.-n. Li, Phys. Rev. D **65**, 074030 (2002); P. Guo, H.-W. Ke, X.-Q. Li, C.-D. Lü and Y.-M. Wang, Phys. Rev. D **75**, 054017 (2007); X.-G. He, T. Li, X.-Q. Li and Y.-M. Wang, Phys. Rev. D **74**, 034026 (2006); Phys. Rev. D **75**, 034011 (2007); C.-D. Lü, Y.-M. Wang, H. Zou, A. Ali and G. Kramer, Phys. Rev. D **80**, 034011 (2009).
- [37] H. Kawamura, J. Kodaira, C.F. Qiao, and K. Tanaka, Phys. Lett. B **523**, 111 (2001); Erratum-ibid. B **536**, 344 (2002).
- [38] B.O. Lange and M. Neubert, Phys. Rev. Lett. **91**, 102001 (2003).
- [39] M. Kobayashi and T. Maskawa, Prog. Th. Phys. **49**, 652 (1973).
- [40] V.M. Braun and I.E. Filyanov, Z Phys. C **48**, 239 (1990); P. Ball, J. High Energy Phys. **01**, 010 (1999).
- [41] P. del Amo Sanchez *et al.* [BABAR Collaboration], Phys. Rev. D **83**, 032007 (2011).
- [42] N. Cundy, M. Gockeler, R. Horsley, T. Kaltenbrunner, A. D. Kennedy, Y. Nakamura, H. Perlt and D. Pleiter *et al.*, Phys. Rev. D **79** (2009) 094507.